

# One-point contact measurement of spherical resonances

C. P. Hsieh and B. Y. Khuri-Yakub

*Edward L. Ginzton Laboratory, Stanford University, Stanford, California 94305-4085*

(Received 1 February 1993; accepted for publication 19 April 1993)

Ceramic bearing balls are desirable for use in high-temperature and nonlubricative environments because of their ability to retain high mechanical strength and reduced wear. However, because ceramics are brittle, it is very important to inspect ceramic parts for the existence of small ( $1\text{--}10\ \mu\text{m}$ ) surface defects. The contact-contact resonant sphere technique has been shown to be able to detect the presence of surface defects in spherical objects. This technique, however, has certain limitations that are especially important when inspecting small spheres. In this letter we present a true one-point-contact technique to circumvent these limitations. We excite resonances of spheres at both low and high frequencies. Resonances are generated by forming a one-point Hertzian contact between the sphere and a spherical depression in a buffer rod with a transducer. The resonance spectrum is detected from the opposite pole of excitation using an optical interferometer. At low frequencies, bulk resonances of the sphere are excited, and material properties are determined. At high frequencies, surface-wave resonances of the sphere are excited, and the dispersion relation of the waves is measured. The measured dispersion relation of the sphere is correlated to the surface wave velocity on the sphere and to the presence of surface defects.

The contact-contact resonant sphere technique<sup>1</sup> is operable in two frequency regions. In the low frequency region, the technique can accurately characterize (one in  $10^4$ ) material acoustic properties such as longitudinal wave velocity, shear wave velocity, and Poisson's ratio.<sup>2</sup> In the high frequency region, where surface wave resonance dominates, it can be used to perform surface defect inspection.<sup>1</sup> The existence of surface defects significantly reduces the quality factor of surface wave resonance modes. However, this technique has its limitations in the alignment of the two transducers, and in controlling the contacting load between the transducers and the sphere. These problems can be circumvented by the following true one-point-contact measurement technique.

Figure 1 shows the schematic of the one-point-contact technique. The sphere is placed on a spherical depression (lens) in a buffer rod with a longitudinal piezoelectric transducer on the other end. The curvature of the lens is less than that of the sphere, so that the sphere can rest at the bottom of the lens. The transducer excites resonances on the sphere and the interferometer measures vertical displacements of the sphere at the opposite pole.

A similar experiment has been performed where a sphere is placed on a three-point mount and resonance is excited photoacoustically by a modulated laser beam.<sup>3</sup> Our technique has several advantages over this earlier technique. First, the only contact between the sphere and the external environment is a single Hertzian contact<sup>4</sup> of which the radius of contact is given by

$$r = F^{1/3} \left( \frac{DRR'}{R - R'} \right)^{1/3},$$

$$D = \frac{3}{4} \left( \frac{1 - \nu^2}{E} + \frac{1 - \nu'^2}{E'} \right),$$

where  $R$ ,  $\nu$ ,  $E$  are the radius, Poisson's ratio, and Young's modulus of the lens, respectively,  $R'$ ,  $\nu'$ ,  $E'$  are the radius, Poisson's ratio, and Young's modulus of the sphere, respectively, and  $F$  is the total contact force (i.e., weight of the sphere).

For example, a fused quartz buffer rod with  $R = 4\ \text{mm}$ ,  $\nu = 0.1694$ ,  $E \approx 7.274 \times 10^{10}\ \text{N/m}^2$ , a 1-mm-diam ceramic ball with  $R' = 0.5\ \text{mm}$ ,  $\nu' \approx 0.2616$ ,  $E' \approx 3.223 \times 10^{11}\ \text{N/m}^2$ , ball density  $\approx 3270\ \text{kg/m}^3$ , we calculate  $r \approx 0.49\ \mu\text{m}$ . At 60 MHz, where the surface wavelength on ceramics is around  $100\ \mu\text{m}$ , the contact diameter is only about 1% of the wavelength, and thus has little effect on the propagation of surface waves.

It is more efficient to excite resonance by a direct mechanical contact; therefore, the measurement is done at a higher signal-to-noise ratio. Furthermore, because the

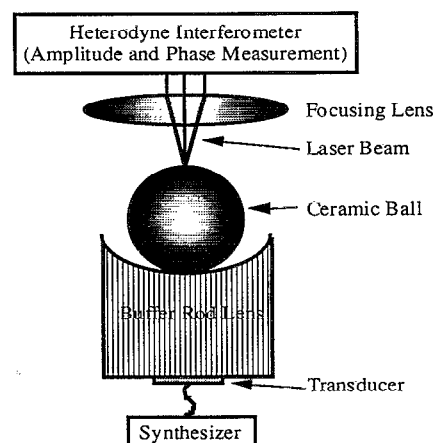


FIG. 1. Schematic of the one-point contact interferometric measurement technique.

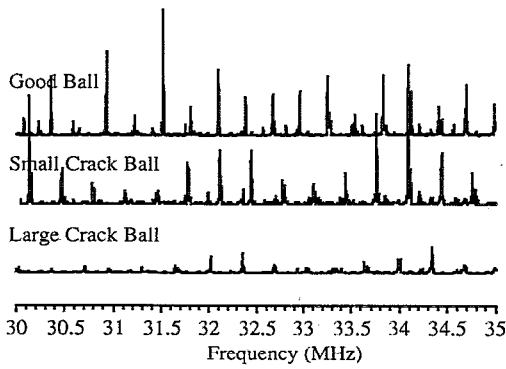


FIG. 2. Amplitude variation with crack size of surface-wave resonant modes. Samples are three  $\text{Si}_3\text{N}_4$  ceramic bearing balls. Diameter = 1/4 in.

sphere is always located at the bottom of the concave lens, alignment of the measurement system for different spheres of identical diameters becomes trivial. Finally, there is no limit to the frequency range over which the measurement can be made.

We measured three  $\text{Si}_3\text{N}_4$  ceramic bearing balls, all with diameters of 1/4 in. One ball was perfect, one had small cracks, and the third had large cracks. We see in Fig. 2 that, as the crack size increases, the resonance energy is scattered, leading to a decrease in resonance amplitude. Figure 3 shows a scrambling effect in the higher frequency range, surface cracks act like secondary sources of propagation of surface waves. The primary wave, generated by the transducer, and the secondary wave, generated by surface cracks, interfere with each other, producing the scrambling effect observed.

We also demonstrated the capability of this technique on small bearing balls. We measured, from 100 kHz to 70 MHz, the resonance spectrum of a  $\text{Si}_3\text{N}_4$  bearing ball with a diameter of 1 mm. In the low frequency spectrum, where we can identify resonant frequencies with bulk resonant modes (torsional or spheroidal),<sup>5</sup> we see that this technique, unlike the contact technique, excites only spheroidal modes. This is because there is only one point of contact, and the excitation direction is in the normal direction of the contact. This also shows the alignment difficulty for the

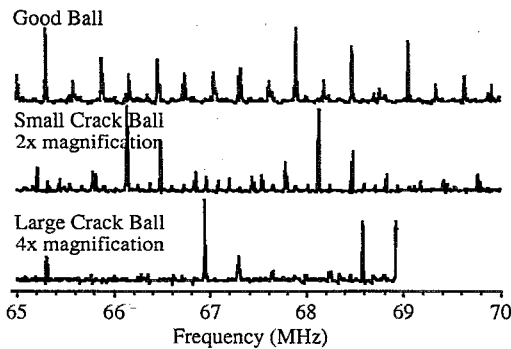


FIG. 3. Scrambling effect of surface-wave resonant modes in the high-frequency range. The interference of primary and secondary waves is apparent.

TABLE I. Material properties of a 1-mm-diam ceramic bearing calculated from two high  $Q$  spheroidal modes.

$\nu$ (Poisson's ratio)	$V_l$ (m/s)	$V_s$ (ms)	$V_R$ (m/s)
0.26646	10999	6206.1	5772.6

contact-contact technique where we did observe torsional modes. We chose two high  $Q$  spheroidal modes to calculate material properties of the 1-mm-diam sphere. The results are shown in Table I. The calculated values of longitudinal and shear wave velocities were then used to calculate the dispersion relation of surface waves. The characteristic equation of spheroidal modes has the form<sup>5</sup>

$$\frac{2\xi}{\eta} \left[ \frac{1}{\eta} + \frac{(n-1)(n+2)}{\eta^2} \left( \frac{J_{n+3/2}(\eta)}{J_{n+1/2}(\eta)} - \frac{n+1}{\eta} \right) \right] J_{n+3/2}(\xi) + \left[ -\frac{1}{2} + \frac{(n-1)(2n+1)}{\eta^2} + \frac{1}{\eta} \right] \times \left( 1 - \frac{2n(n-1)(n+2)}{\eta^2} \right) \frac{J_{n+3/2}(\eta)}{J_{n+1/2}(\eta)} J_{n+1/2}(\xi) = 0,$$

where

$$\eta = \frac{2\pi f R'}{V_s},$$

$$\xi = \frac{2\pi f R'}{V_l},$$

$f$  is the operating frequency,  $R'$  is the radius of the sphere,  $V_s$  is the shear wave velocity of material of the sphere,  $V_l$  is the longitudinal wave velocity of the material of the sphere, and  $n$  is a positive integer.

Solutions for  $n=0$  correspond to longitudinal wave resonance modes. The first solution of each positive integer  $n$  corresponds to surface wave resonance modes (there is no surface wave resonance mode solution for  $n=1$ ). For  $n$  larger than 100, the equation asymptotically approaches that of the Rayleigh wave characteristic equation.

The apparent surface wave velocity  $V_R$  is calculated as follows:

$$m = \frac{2\pi R'}{\lambda_R} = \frac{2\pi R' f}{V_R},$$

therefore

$$V_R = \frac{2\pi R' f}{m},$$

where  $m=n+2$  is the number of waves on the sphere.

This calculated surface-wave dispersion curve is then compared to the experimentally measured surface wave resonances, as seen in Fig. 4. We see that the apparent surface wave velocity asymptotically approaches a constant, true Rayleigh wave velocity.

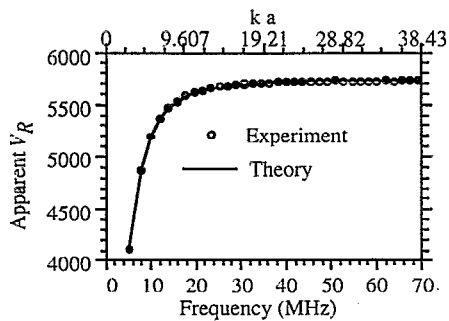


FIG. 4. Dispersion relation of surface waves on a sphere. Note that  $V_R$  used in the upper horizontal axis is the true Rayleigh wave velocity.

We have developed and demonstrated a new technique capable of measuring the material properties of spherical objects, and of inspecting them for the presence of surface defects. The technique uses a single point contact to excite resonances in the object and an optical interferometer to measure these resonances. The measurement is capable of

measuring material properties and detecting the existence of surface defects, and the measurements are reproducible. The measurement can be made on spherical objects of any size and over an unlimited frequency range. We also showed, for the first time, good agreement between theory and experiment for the dispersion relation of surface waves on a sphere. This technique has the potential of inspecting nonmetallic spheres, or spheres with coatings, and cylindrical objects. It can also be applied to objects of uncommon geometries.

This work was supported by the Department of Energy under Contract No. DE-FGO3-84ER45157.

- <sup>1</sup>C. P. Hsieh and B. T. Khuri-Yakub, *Appl. Phys. Lett.* **60**, 1815 (1992).
- <sup>2</sup>D. B. Fraser and R. C. LeCraw, *Rev. Sci. Instrum.* **35**, 1113 (1964).
- <sup>3</sup>Y. Shui, D. Royer, E. Dieulesaint, and Z. Sun, in *IEEE 1988 Ultrasonics Symposium Proceedings*, Chicago, Illinois, edited by B. R. McAvoy (Institute of Electrical and Electronics Engineers, New York, 1988), p. 343.
- <sup>4</sup>S. P. Timoshenko and J. N. Goodier, in *Theory of Elasticity*, 3rd ed. (McGraw-Hill, New York, 1970), p. 409.
- <sup>5</sup>Y. Sato and T. Usami, *Geophys. Mag.* **31**, 25 (1962).